a small sample is a big step forward in analytical capability.

Crystal-structure refinement of amphiboles that have a completely ordered cation distribution at the octahedral sites [tremolite(30), fluor-richterite(34), fluor-tremolite(36), tremolite (56a, b)] indicates that the isotropic temperature-factors at the three octahedral sites are approximately equal. This also appears to be the case for amphiboles with cation disorder at the octahedral sites [grunerite(22), ferro-tschermakite(54), potassium-arfvedsonite(67)]. This suggests that the isotropic temperature-factors at the octahedral sites provide an independent check on the refined site-populations. Two factors can give rise to incorrect site-populations: (i) systematic error in the diffraction data and (ii) incorrect linear constraints during site-population refinement. The effects of the second factor have not been investigated at all.

In summary, site populations may be derived directly from diffraction data where two cation species differ significantly in scattering power and are disordered over two or more sites. Any additional information must be derived from indirect methods, such as the mean bond-length – constituent-cation-radius relationships developed in the previous sections. Experimental results on published refinements of amphibole, together with a critical assessment of their probable accuracy, are given in Appendices A3, B3, C3 and D3.

MÖSSBAUER SPECTROSCOPY OF AMPHIBOLES

The Mössbauer effect is the recoil-free emission and resonant absorption of gamma rays by a specific atomic nucleus. Of the thirty or so isotopes sensitive to this effect, only ^{57}Fe is of use in amphibole studies; however, the almost ubiquitous occurrence of Fe^{2+} and Fe^{3+} has resulted in the application of this technique to a wide variety of amphiboles. Introductions to the theory and application of Mössbauer spectroscopy are given by Wertheim (1964), Frauenfelder (1962), Fluck (1964) and Bancroft (1973), and a general discussion of the problems inherent in the derivation of site populations is given by Hawthorne (1983).

The hyperfine parameters of amphiboles show significant variation with changes in co-ordination, site occupancy and compositional type. The systematics of these variations are of interest both with regard to peak assignment in Mössbauer spectra and the crystal-chemical

systematics of the amphiboles themselves. Some of the general conclusions of Ingalls (1964) concerning the behavior of the quadrupole splitting of high-spin Fe^{2+} with changes in ligand environment are pertinent. In particular, Fe^{2+} in a cubic field has no quadrupole splitting; slight distortion of the field from cubic symmetry produces a large quadrupole-splitting ($\sim$3.7 mm/s), with increasing distortion of the ligand environment producing a gradual decrease in the quadrupole splitting. The crystal-field contribution to the quadrupole splitting contains both distance and angular terms and hence is sensitive to distortion of the co-ordination poly-hedron with regard to both bond lengths and bond angles. Consequently, the criterion by which distortion is measured should encompass both these factors; failure to do so has led to some confusion in discussions relating Mössbauer parameters to crystal structure. Next-nearest-neighbor cations will also have a significant effect on the quadrupole splitting. This is of particular importance in the amphiboles, where coupled polyvalent cation-substitutions at the M(2), M(4), T(1), T(2) and A sites are particularly common.

Perhaps the first applications of this method to amphiboles occurred in the oxidation studies of fibrous amphiboles by Gibb & Greenwood (1965). However, precise site-populations were not obtained until the introduction of least-squares refinement to the analysis of complex spectra (Stone 1967). This led to more quantitative estimates of site populations in amphiboles (Bancroft 1967), and systematic studies of amphiboles were soon appearing (Bancroft et al. 1966, 1967a, b, Bancroft & Burns 1968).

In most site-population studies of amphiboles, it is necessary to apply linear constraints during the least-squares-fitting procedure in order to attain convergence. These constraints are usually of two types: (i) equal-half-width constraints, and (ii) equal-area constraints.

The equal-half-width constraints are justified on the grounds that the component peaks of ferrous doublets representing iron in different sites have uniform half-widths in numerous minerals (Burns & Greaves 1971); hence this is justified empirically. This is perhaps overstating the case, as there are several reasons why unequal half-widths can be encountered in spectra from complex minerals. Variation in nearest-neighbor (anion) and next-nearest-neighbor (cation) site-occupancy can produce an increase in the half-width of the corresponding peak. Similarly, overlap of two or more peaks can lead to an apparent single peak with a slightly

larger half-width than usual. This is the case with the spectra of the cummingtonite – grunerite series (Bancroft et al. 1967a, Ghose & Hafner 1969, Hafner & Ghose 1971), where the component peaks of the doublets representing Fe^{2+} in M(1), M(2) and M(3) overlap almost perfectly to give a multiple peak with a half-width only slightly larger than that of the doublet due to Fe^{2+} at M(4). Unequal half-widths can also be produced during the least-squares-fitting procedure by using inappropriate linear constraints and the resulting parameter-interaction during refinement. If equal-area constraints are applied when the lower velocity absorption is greater than the higher velocity absorption in an amphibole containing both Fe^{2+} and Fe^{3+}, then the Fe^{2+} contribution to the lower velocity envelope will not be sufficient and the Fe^{3+} doublet will increase in both intensity and half-width (particularly the latter) to compensate for this incorrectly imposed constraint. Where Fe^{3+} doublets with large half-widths have been encountered in previous studies, it has been the practice to explain this by proposing the occurrence of Fe^{3+} in all octahedral sites, with the Fe^{3+} "doublet" actually being an overlap of several doublets. This may well be the case in some instances; however, other explanations are possible, and this does not constitute proof for Fe^{3+} occupancy of M(1) or M(3) (or both) without additional evidence. For example, if all Fe^{2+} peaks are constrained to be of equal half-width, any slight inaccuracies in this assumption together with other "slop" in the model will be compensated for in the half-width of the Fe^{3+} peaks, which thus will frequently be wider than the derived Fe^{2+} peaks.

Despite the improvement in resolving spectra that occurred as a result of the application of least-squares techniques, resolution is still a problem in amphibole studies. One technique that has had some success in other mineral groups is to vary the absorber temperature. This does not appear to be of much use in the amphiboles as change in absorber temperature appears to result in increased resolution in the upper velocity envelope and decreased resolution in the lower velocity envelope with little or no net change in the resolution of the individual spectral components.

The question of resolution and accuracy has been virtually ignored in most Mössbauer studies of site populations in amphiboles. Many studies refer to the discussion given by Bancroft (1970)

TABLE 52. TYPICAL CORRELATION MATRIX FROM A LEAST-SQUARES REFINEMENT CYCLE OF AN AMPHIBOLE MÖSSBAUER SPECTRUM

	1	2	3	4	5	6	7	8	9	10	11	12	13	14	15	16	17	18
P1	-0.08	0.08	0.20															
	0.05	-0.12	-0.05															
W1	-0.27	0.38	0.44	0.25														
	-0.01	-0.04	-0.01	0.85														
A1	-0.48	0.71	0.50	0.17	0.65													
	0.04	-0.13	-0.12	0.85	0.94													
P2	0.05	-0.06	-0.15	-0.18	-0.53	-0.13												
	0.09	-0.18	-0.16	0.79	0.74	0.84												
W2	-0.27	0.38	0.40	0.56	0.55	0.60	-0.14											
	-0.07	0.20	0.19	-0.63	-0.80	-0.92	-0.68											
A2	-	-	-	-	-	-	-	-										
	-0.05	0.16	0.15	-0.74	-0.90	-0.97	-0.74	0.98										
P3	0.04	-0.07	-0.11	-0.09	-0.27	-0.15	-0.09	-0.49	-									
	0.02	-0.03	0.03	0.14	0.00	-0.00	0.16	0.10	-0.11									
W3	-0.21	0.33	0.24	0.19	0.28	0.54	0.30	0.35	-	-0.11								
	-0.20	0.36	0.07	-0.14	-0.15	-0.17	-0.03	0.21	0.18	0.04								
A3	-	-	-	-	-	-	-	-	-	-	-							
	-0.30	0.53	0.06	-0.13	-0.08	-0.12	-0.06	0.17	0.14	-0.02	0.72							
P4	-0.02	0.00	-0.03	-0.11	-0.20	-0.08	0.12	-0.20	-	0.02	-0.39	-						
	0.03	0.01	0.08	-0.31	-0.49	-0.56	-0.24	0.69	0.68	0.10	-0.17	-0.02						
W4	-0.19	0.26	0.24	0.27	0.21	0.39	0.03	0.33	-	0.28	0.30	-	-0.11					
	-0.13	0.06	0.14	0.37	0.53	0.58	0.26	-0.69	-0.69	-0.10	-0.15	-0.23	-0.74					
A4	-	-	-	-	-	-	-	-	-	-	-	-	-	-				
	-0.04	-0.06	-0.02	0.45	0.66	0.75	0.39	-0.89	-0.87	-0.28	-0.20	-0.23	-0.80	0.89				
P5	-0.10	0.12	0.11	0.05	0.07	0.18	0.04	0.07	-	0.06	0.08	-	0.13	0.11	-			
	-0.11	0.11	0.17	0.05	0.07	0.05	0.01	-0.04	-0.05	0.00	-0.01	0.00	0.00	0.17	0.11			
P6	0.13	-0.14	-0.15	0.06	-0.01	-0.11	0.01	0.06	-	-0.11	-0.03	-	-0.04	-0.12	-	-0.02		
	0.02	-0.11	-0.06	0.29	0.47	0.54	0.19	-0.70	-0.69	-0.40	-0.13	-0.16	-0.74	0.75	0.86	0.08		
P7	0.09	-0.09	0.06	-0.02	-0.01	-0.01	-0.25	-0.01	-	-0.15	-0.04	-	-0.06	-0.28	-	-0.03	0.34	
	-0.06	0.13	0.15	-0.84	-0.80	-0.88	-0.92	0.70	0.77	-0.23	0.11	0.04	0.27	-0.29	-0.41	0.00	-0.17	
P8	0.15	-0.24	-0.10	-0.32	-0.16	-0.27	-0.01	-0.55	-	0.26	-0.18	-	0.10	-0.19	-	-0.03	0.05	0.10
	-0.02	0.08	0.11	-0.88	-0.90	-0.94	-0.85	0.78	0.87	-0.02	0.10	0.04	0.44	-0.45	-0.59	-0.03	-0.39	0.89

P   peak position, W = half-width, A = area

concerning these factors; based on a peak width at half-height (half-width) of 0.30 mm/s, (i) peaks closer than half the half-width (~0.15 mm/s) cannot be resolved, (ii) peaks ~0.20 mm/s apart are just resolvable, and hence the site populations will have very large (>15%) standard deviations, and (iii) peaks ≧0.30 mm/s apart are easily resolved and the site populations will have reasonable (<10%) standard deviations. These figures were presumably given as a rough guide and do not take the place of a calculated standard deviation.

Statistical tests are used as a measure of comparison between alternate models, with the residual as a measure of the agreement between the observed data and a corresponding set of calculated data derived from the least-squares solution. Statistical acceptability and a low residual are no guarantee that the derived model is correct. The most obvious example of this are the Mössbauer spectra of the amphiboles of the magnesio-cummingtonite–grunerite series (Bancroft *et al.* 1967a, Hafner & Ghose 1971); statistically acceptable fits consist of two quadrupole-split Fe^{2+} doublets when the crystal structure indicates that the correct model should consist of four Fe^{2+} doublets. In the absence of other criteria, the simpler of two solutions is to be preferred (Law 1973). However, if additional information is available, the solution consonant with this is to be preferred.

The major problem encountered in the fitting of most amphibole spectra is high correlation between parameters in the least-squares procedure. This problem has been examined by Hawthorne (1973), using amphiboles already characterized by crystal-structure refinement. It was found that application of area constraints derived from the X-ray site populations together with equal half-width constraints for all lines or equal doublet half-widths led to acceptable R_o values. Removal of the area constraints led to changes in area ratios that in some cases bore no resemblance to the X-ray results at all, and in significantly different half-widths for different doublets. The good agreement between the X-ray site-population results and the Mössbauer data suggests that the unconstrained (no X-ray-derived area constraints) least-squares fitting procedure is giving spurious results. Examination of the correlation matrix after each spectrum refinement reveals large interparameter correlations. A typical correlation-matrix (both with and without X-ray area-constraints) is shown in Table 52; for the matrix with X-ray area-constraints, the largest element is $|0.71|$ and 8 elements exceed $|0.5|$, whereas for the unconstrained refinement, the largest matrix element is $|0.98|$ and 51 elements exceed $|0.5|$. Obviously the normal equations matrix is extremely ill-conditioned, with variable correlation significantly affecting the refined parameters. If the standard deviations are calculated from the full matrix, they will reflect this high correlation; if they are calculated using the diagonal approximation, the standard deviations will be unrealistically low (*cf.* Table 51). However, most amphibole studies do not include standard deviations for their site populations; this makes the significance of the results
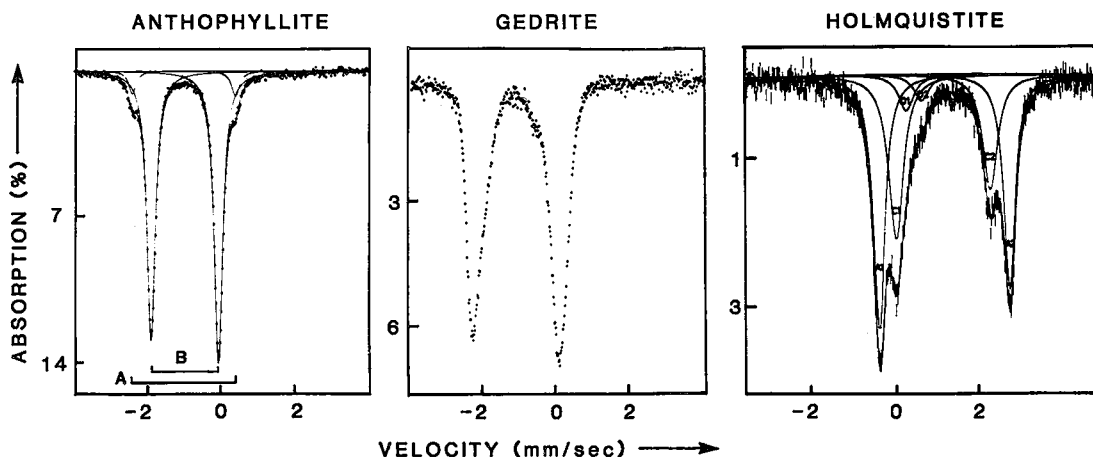

FIG. 63. Room-temperature Mössbauer spectra of anthophyllite (left), gedrite (centre), both from Seifert (1977), and holmquistite (right), from Law (1973).

hard to evaluate on a quantitative basis. This is probably not as serious a deficiency in these studies as first appears, as it is probable that the standard deviations are not too useful in these particular cases. This is illustrated by the site populations and associated standard deviations derived from the refinement of Table 52. The difference between the two sets of site occupancies is highly significant in terms of the correctly calculated standard deviations. This apparently anomalous result occurs because we are performing a linear hypothesis test in a very nonlinear region of parameter space. There seems to be no general solution to this problem (Beale 1960); however, such a standard deviation is useful as a minimum estimate when it is known that this problem does occur.

The general appearance of amphibole Mössbauer spectra varies considerably with amphibole type, and the peak assignment in these spectra is frequently not straightforward. As a result, it is necessary to consider the systematics of the Mössbauer parameters to ensure correct peak assignment. A general survey follows, and quantitative results are given in Appendix F.

Fe–Mg–Mn amphiboles

Typical spectra for the orthorhombic Fe–Mg–Mn amphiboles are shown in Figure 63. The anthophyllite spectrum consists of two doublets; the outer doublet is attributable to Fe^{2+} at the M1, M2 and M3 sites, with the inner doublet due to Fe^{2+} at the M4 site. This contrasts with the gedrite spectrum, where only a single wide doublet occurs. The reason for this is apparent in the systematics of the quadrupole splittings for these amphiboles as shown in Figure 64. Extrapolation of the quadrupole-splitting values for the M4 and M1+M2+M3 peaks in the anthophyllite spectra to Al values typical of gedrite shows that the Q.S. values overlap, with a concomitant lack of resolution in the gedrite spectra (Seifert 1977).

The holmquistite spectrum consists of three doublets that may be assigned to Fe^{3+} at the
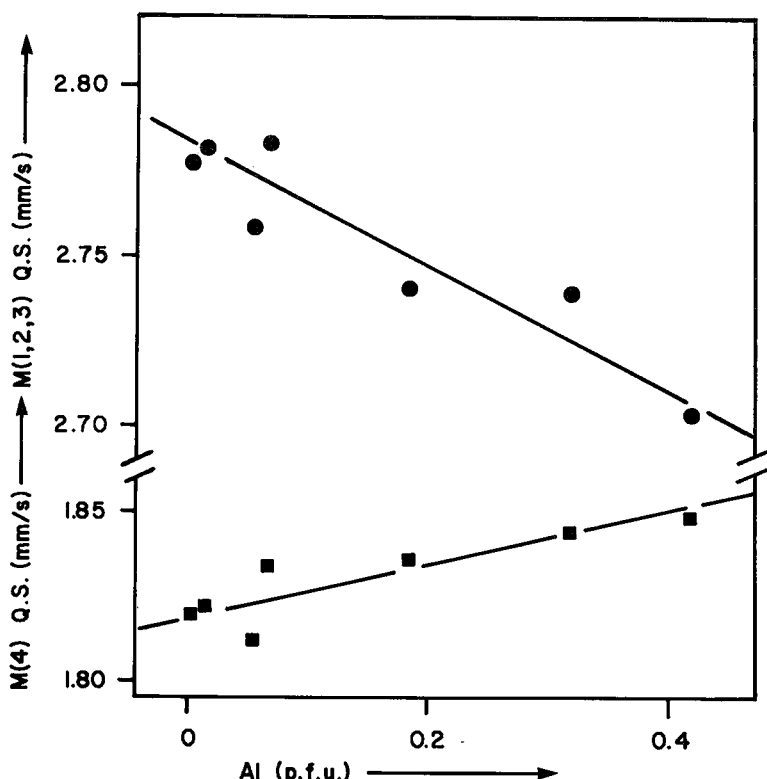
FIG. 64. Quadrupole splitting (at room temperature) as a function of Al p.f.u. in orthorhombic amphiboles [after Seifert (1977)].

MAGNESIO-CUMMINGTONITE
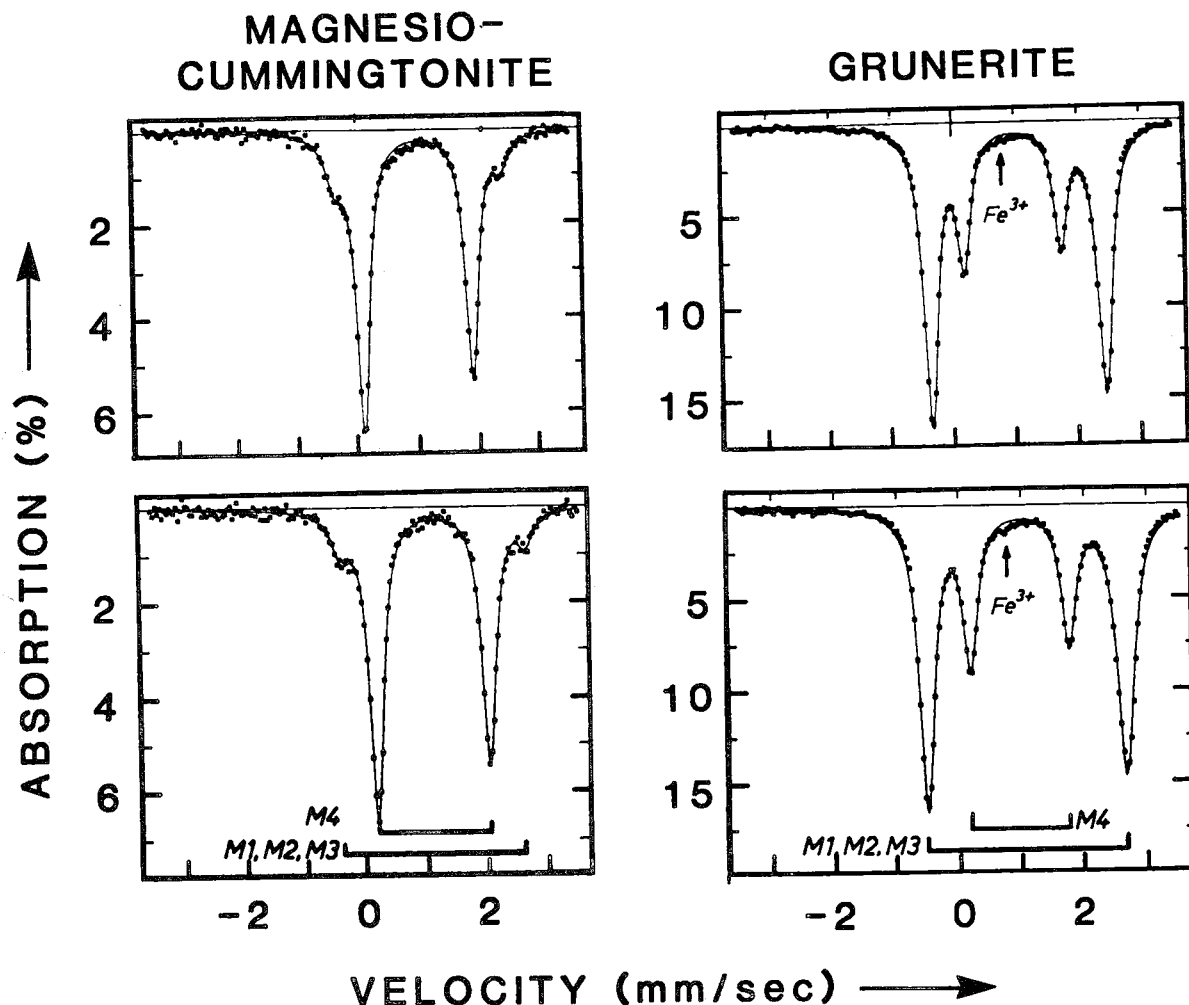
GRUNERITE

FIG. 65. Room-temperature (upper) and liquid-nitrogen-temperature (lower) Mössbauer spectra of magnesio-cummingtonite (left) and grunerite (right) [from Hafner & Ghose (1971)].

M2 site (D1, D2) and Fe^{2+} at the M1 (A1, A2) and M3 (C1 and C2) sites. The resolution of the spectrum is similar to that in the glaucophane – riebeckite group.

Typical Mössbauer spectra for the monoclinic Fe–Mg–Mn amphiboles are shown in Figure 65; slightly greater resolution is attained in low-temperature spectra, a feature also exhibited by the anthophyllite spectra. The spectra are similar to the anthophyllite spectra, with the outer and inner doublets assigned to Fe^{2+} at the M(1)+M(2)+M(3) and M(4) sites, respectively. Perhaps the most notable feature of the Fe–Mg–Mn amphibole spectra is the complete overlap of doublets due to Fe^{2+} at the

M(1), M(2) and M(3) sites. At first sight, this appears to be incompatible with the fact that these amphiboles show considerable differences in nearest- and next-nearest-neighbor configurations between these three sites. However, there is an inverse relationship between the distance (Δ) and angle (σ^2) distortion parameters for nonaluminous compositions (Fig. 66). One may surmise that the differences in angular distortion at the M(1), M(2) and M(3) sites are compensated for by the differences in bond-length variations, with the result that the quadrupole splittings at the various sites are very similar. This will be enhanced by the occupancy of the four M sites by $Mg+Fe^{2+}+$
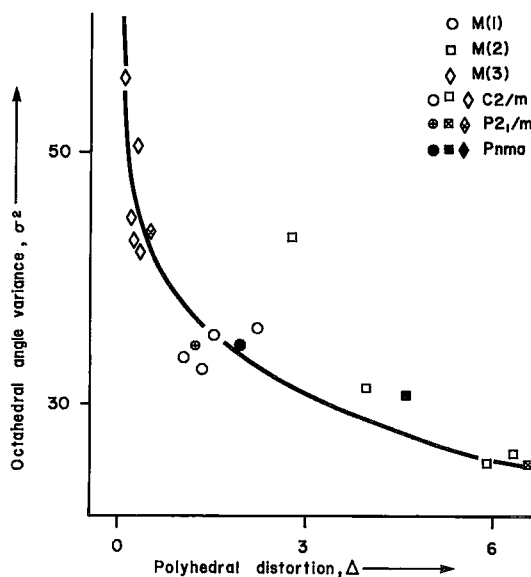
FIG. 66. Variance in octahedral angle as a function of polyhedral distortion for the M(1), M(2) and M(3) sites in the Fe–Mg–Mn amphiboles.

Mn only, leading to as similar a next-nearest-neighbor environment for the M(1), M(2) and M(3) sites as is possible in the amphibole structure. If this is the case, the question then arises as to why does not this complete overlap occur in other amphibole series. Several studies have suggested that this is due to the greater variation in next-nearest-neighbor character, with Ca and Na occupying the M(4) site and Al and Fe^{3+} occupying the M(2) site. In addition to these considerations, some amphiboles types do not show an inverse correlation of angular distortion and bond-length variation at the M(1,2,3) sites.

Several studies have examined the variation in quadrupole splitting with composition in the Fe–Mg–Mn amphiboles. Bancroft et al. (1967b) showed a linear decrease in the Q.S. of Fe^{2+} at M(4) with increasing Fe/(Fe+Mg) in amphiboles of the cummingtonite – grunerite series, which is further supported by the work of Barabanov & Tomilov (1973) and Goldman (1979). Barabanov & Tomilov (1973) also showed that the I.S. of Fe^{2+} at M(4) gradually decreases with increasing Fe/(Fe+Mg) in this series. For the data of Appendix F, these relationships are shown in Figure 67. The quadrupole splitting of Fe^{2+} at M(4) is negatively correlated with the Fe/(Fe+Mg) ratio of the amphibole, a slight nonlinearity in

the relationship being apparent, particularly at low Fe/(Fe+Mg) ratios if the orthorhombic amphiboles are included in the correlation. The correlation is perhaps improved slightly if the M(4) Fe^{2+} quadrupole splitting is plotted against the mean Fe/(Fe+Mg) content of the M(1), M(2) and M(3) sites. This is in line with the suggestion of Hafner & Ghose (1971) that the octahedral distortions, and thence the quadrupole splittings, are dictated not by the site occupancy of the specific site but by the linkage between the octahedral and tetrahedral parts of the structure. Certainly the geometry of the M(4) site in the monoclinic amphiboles is consonant with this suggestion. Figure 68 shows the variation in M(4) polyhedral distortion Δ with the mean Fe/(Fe+Mg) content of the M(1), M(2) and M(3) sites; the regular increase in distortion with increasing Fe/(Fe+Mg) correlates with the decreasing quadrupole splitting of Fe^{2+} at M(4), in agreement with the conclusions of Ingalls (1964). Note that the orthorhombic amphiboles have not been included in Figure 68 because of the differences in co-ordination of the M4 site, which appears to be [7] or [5] in anthophyllite. There is a significant decrease in the isomer shift of Fe^{2+} at M(4) with increasing Fe/(Fe+Mg) at M(1), M(2) and M(3); this decrease in isomer shift hence is negatively correlated with increasing distortion of the M(4) polyhedron. Decreasing isomer-shift is indicative of increased covalent character of the bonding. Brown & Shannon (1973) have suggested that the degree of covalent character of a chemical bond between a specific pair of chemical species is a function of its length, shorter bonds being more covalent than longer bonds. This being the case, increased polyhedral distortion (relative deviation of bond lengths from the mean value) will result in an increase in mean bond-length *and* average bond-covalency. Thus the decreasing isomer-shift of Fe^{2+} at M(4) with increasing Fe/(Fe+Mg) at the M(1), M(2) and M(3) sites is a result of the increased covalent bonding of Fe^{2+} at M(4) due to the increased polyhedral distortion of the M(4) polyhedron. There seems to be no systematic variation in quadrupole-splitting and isomer-shift values of Fe^{2+} at the M(1), M(2) and M(3) sites in the monoclinic Fe–Mg–Mn amphiboles. The large quadrupole-splitting values are consonant with the regularity of the M(1), M(2) and M(3) sites when compared with the corresponding values for Fe^{2+} at the M(4) site.

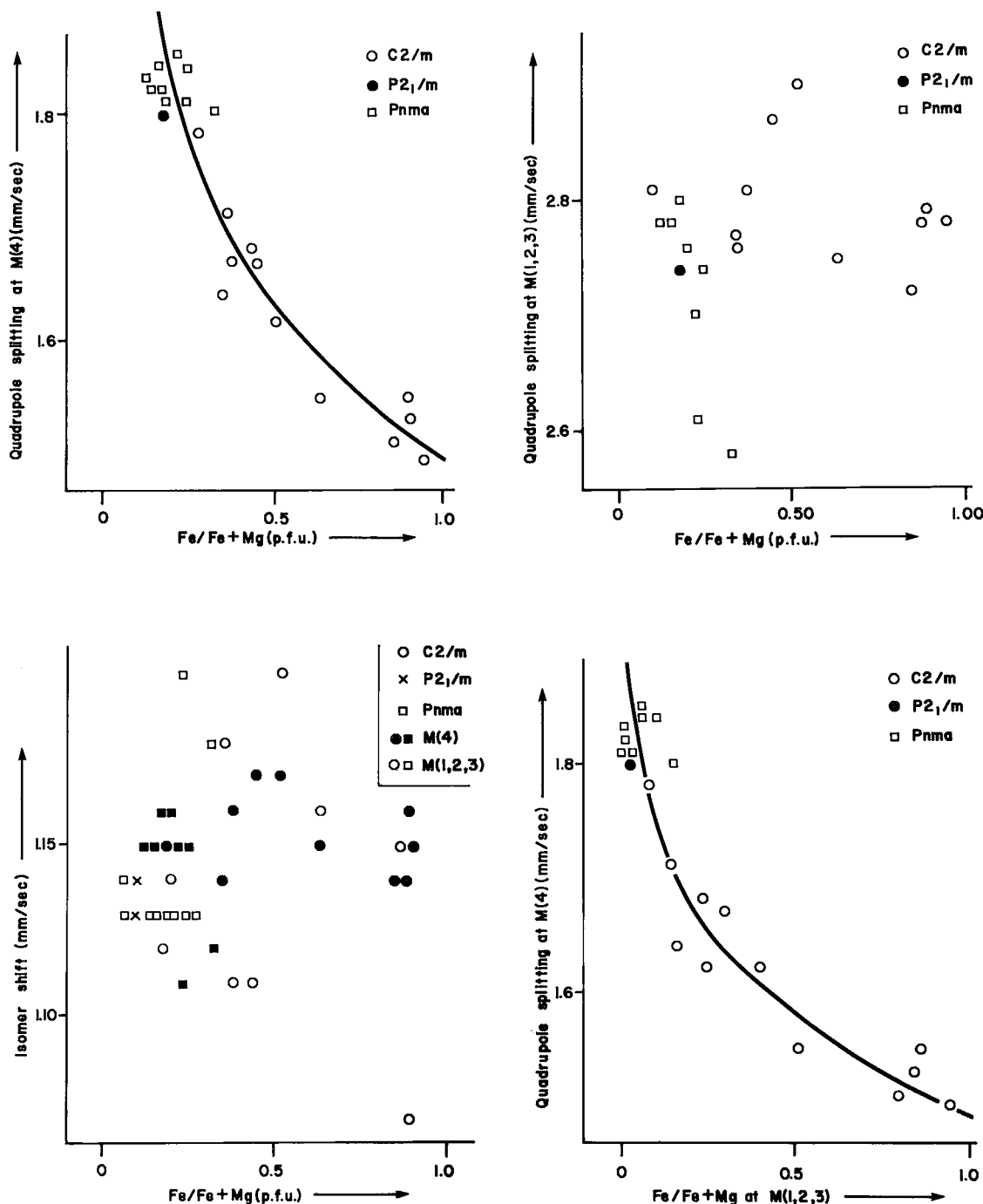The above discussion concerning the covalency of Fe^{2+} at M(4) would suggest that the

FIG. 67. Compositional systematics of the Mössbauer parameters in the Fe–Mg–Mn amphiboles. Values of isomer shift are relative to metallic Fe.

isomer-shift values of Fe^{2+} at M(1), M(2) and M(3) should be larger than the values for the corresponding doublet due to Fe^{2+} at M(4) and this does hold for all of the other data. Hafner
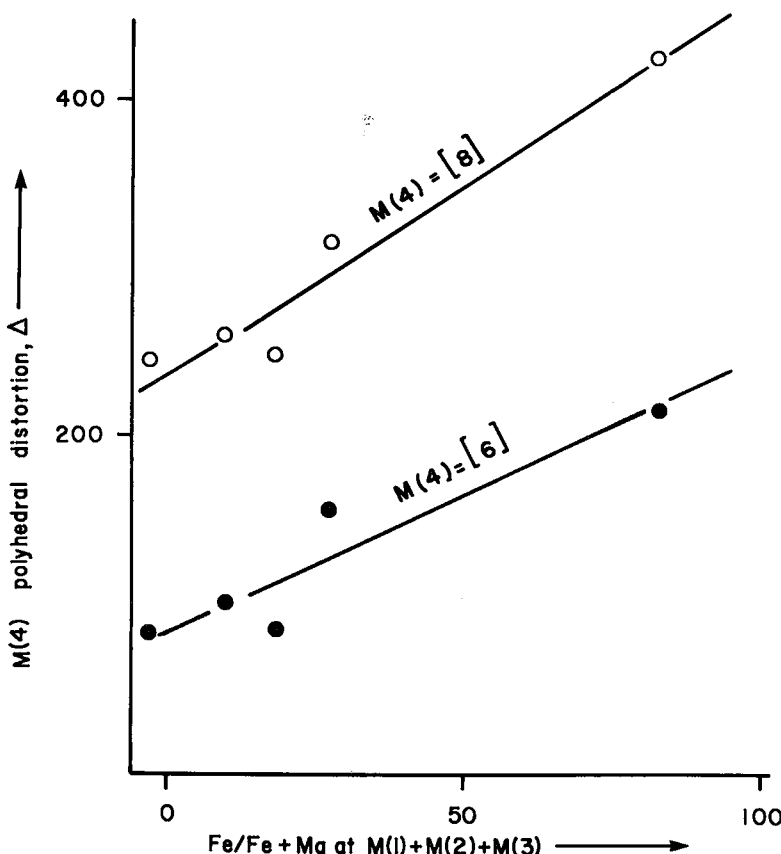
FIG. 68. M(4) polyhedral distortion as a function of composition for the monoclinic Fe–Mg–Mn amphiboles.

& Ghose (1971) noted that in chain silicates, the site with the stronger octahedral distortion has smaller Fe^{2+} isomer shifts and a higher covalent component in the bonding, with Fe^{2+} at M(4) being more covalent than Fe^{2+} at M(1), (2) and M(3) in cummingtonite.

Systematic variation of hyperfine parameters in the orthorhombic amphiboles has been examined in detail by Seifert (1977). The actual values of quadrupole splitting and isomer shift are fairly similar to corresponding values in the monoclinic Fe–Mg–Mn amphiboles, but show slightly more variation due to the wider variations in chemistry that can be encountered in the orthorhombic amphiboles. Figure 64 shows the variation in quadrupole splitting of Fe^{2+} at the M4 and M1+M2+M3 sites in a series of anthophyllite specimens. It was shown in an earlier section that the angular distortion of the M1 and M3 octahedra are inversely correlated with the mean ionic radius of the cations occu-

pying the M2 site (Fig. 52). The decrease in quadrupole splitting of Fe^{2+} at M1, M2 and M3 with increasing Al content may thus be due to an increase in distortion of the M1 and M3 octahedra, together with an increase in the mean cation charge of the next-nearest octahe-drally co-ordinated cations. Accompanying this decrease in quadrupole splitting is an increase in line width that is indicative of increasing difference between the M1, M2 and M3 sites when occupied by Fe^{2+}. Although the quadru-pole splitting of Fe^{2+} at M4 conforms to the trend shown by the monoclinic Fe–Mg–Mn amphiboles (Fig. 68), there is a significant variation in quadrupole splitting, being positively correlated with the increase in total Al (Fig. 64). This increase in quadrupole splitting suggests a decrease in distortion of the M4 polyhedron (Seifert 1977), in agreement with the fact that the M4 polyhedron is far more regular in gedrite than in anthophyllite. The systematic
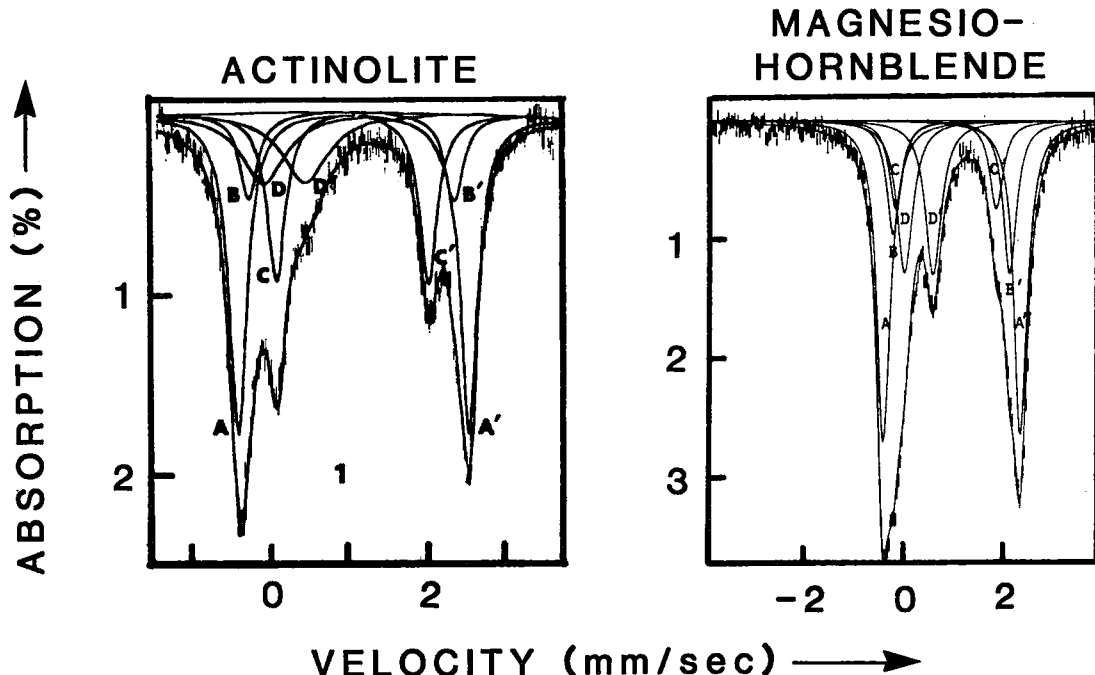
FIG. 69. Room-temperature Mössbauer spectra of actinolite (left) and magnesio-hornblende (right) [from Burns & Greaves (1971) and Bancroft & Brown (1975), respectively]. The doublets are assigned as follows: AA', Fe^{2+} at M(1); BB', Fe^{2+} at M(2); CC', Fe^{2+} at M(3); DD', Fe^{3+} predominantly at M(2).

variation of hyperfine parameters with composition in anthophyllite (Seifert 1977) helps to clarify the Mössbauer spectrum of gedrite, which shows a single broad doublet of asymmetric peaks that cannot be resolved into component peaks. If the trends exhibited by Figure 64 continue to homogeneous gedrite compositions, strong overlap of the two doublets would occur, as appears to be the case. In agreement with the discussion given for monoclinic Fe–Mg–Mn amphiboles, the isomer shift of Fe^{2+} at M4 is slightly smaller than the isomer shift of Fe^{2+} at M1, M2 and M3, suggesting that the bonding is slightly more covalent in the more distorted M4 polyhedron.

The calcic amphiboles

The interpretation of the Mössbauer spectrum of calcic amphiboles is not straightforward, and peak assignments differ from study to study. Burns *et al.* (1970) resolved four quadrupole-split doublets in the spectrum of actinolite samples, assigning them to Fe^{2+} at M(1), M(2) and M(3), respectively, and Fe^{3+} at all octahedrally co-ordinated sites. Burns & Greaves (1971) also resolved actinolite spectra into four quadrupole-split doublets (Fig. 69), but used a

different site-assignment for the doublets. Bancroft & Brown (1975) resolved the spectra of a series of hornblendes into four quadrupole-split doublets (Fig. 69); however their association of the individual peaks into doublets differed from that of Burns & Greaves (1971). Goodman & Wilson (1976) resolved the spectrum of a hornblende into five quadrupole-split doublets due to Fe^{2+} at M(1), M(2), M(3) and M(4) together with an Fe^{3+} doublet (Fig. 70). Goldman & Rossman (1977a) presented the Mössbauer spectrum of a tremolite (Fig. 71) with two quadrupole-split doublets only, and put forward evidence in the form of electronic absorption spectra that the two doublets represented Fe^{2+} at M(4) (doublet BB') and M(1)+M(2)+M(3) (doublet AA'); Goldman (1979) has provided additional arguments supporting this assignment. As the Fe^{2+} contents of M(4) in amphiboles of the tremolite – ferroactinolite series are low, any doublet due to Fe^{2+} at M(4) should be swamped out in ferroactinolite by greatly increased response from Fe^{2+} at the M(1), M(2) and M(3) sites; Goldman (1979) shows that this is indeed the case.
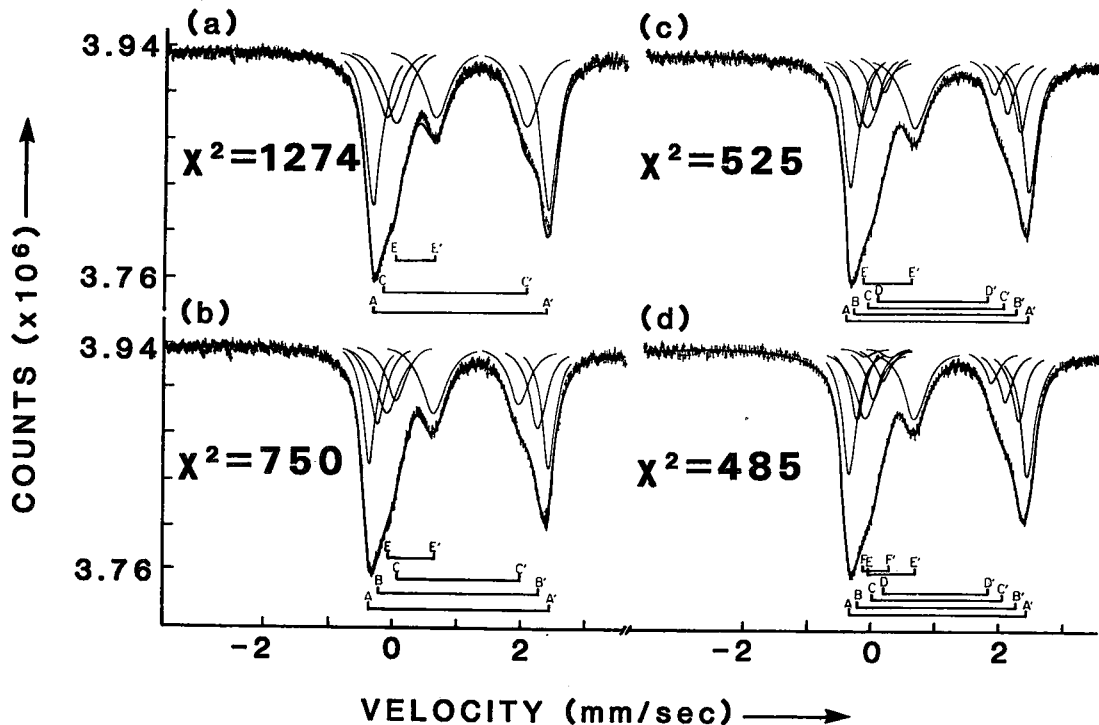
Goldman (1979) has proposed that the peak

FIG. 70. Room-temperature Mössbauer spectrum of hornblende; (a) 3-doublet fit; (b) 4-doublet fit; (c) 5-doublet fit; (d) 6-doublet fit. Peak assignments are as follows: AA′, BB′, CC′, DD′: Fe^{2+} at M(1), M(2), M(3) and M(4), respectively; EE′, FF′: octahedrally and tetrahedrally co-ordinated Fe^{3+}, respectively [from Goodman & Wilson (1976)].

assignment in previous studies of actinolite be altered as follows AA′ = M(1)+M(3), BB′ = M(2), CC′ = M(4); in some cases, this is supported by evidence from electronic absorption spectra. This argument is based on: (i) the Q.S. value for the CC′ doublet (~1.8 mm/s) is similar to M(4) doublet values in the Mg–Fe–Mn amphiboles, (ii) comparison of amphibole spectra with corresponding pyroxene spectra, (iii) stoichiometric indications that C-type cations must occur at the M(4) site in the calcic amphiboles examined, and (iv) systematics of the hyperfine parameters in amphiboles.

Inspection of the stoichiometry of the hornblendes examined by Bancroft & Brown (1975) indicates that any spectral contribution from Fe^{2+} at M(4) should be negligible compared with the contributions from iron at the octahedrally co-ordinated sites. The systematics of the hyperfine parameters are examined in Figure 72. There is an increase in the quadrupole splitting for Fe^{2+} at M(1) and M(3) with increasing M(2) cation size; although the trend

is not well developed, it does fit the correlation exhibited by Fe^{2+} at the M(3) site in the alkali amphiboles (Fig. 75), and supports the arguments of Goldman (1979) outlined above. Goldman (1979) also showed that the quadrupole splitting of Fe^{2+} at M(1) in these data correlates well with the total content of trivalent cations in the amphibole (Fig. 73); however, inclusion of the magnesio-hastingsite{67} data of Semet (1973) spoils this trend. The available data on actinolite tend to agree with the trends presented by Goldman (1979) and in this study, but striking deviations do occur. The fact that improved correlations result when the total trivalent cation content is used suggest that tetrahedrally co-ordinated Al has an important role in affecting the quadrupole splitting of Fe^{2+} at the M(1) site (Goldman 1979). However, whether this is an inductive effect through the linkage requirements of the octahedral strip and tetrahedral chain elements (Hawthorne 1979) or a direct change in the crystal-field component from the next-nearest-neighbor cations is not clear.
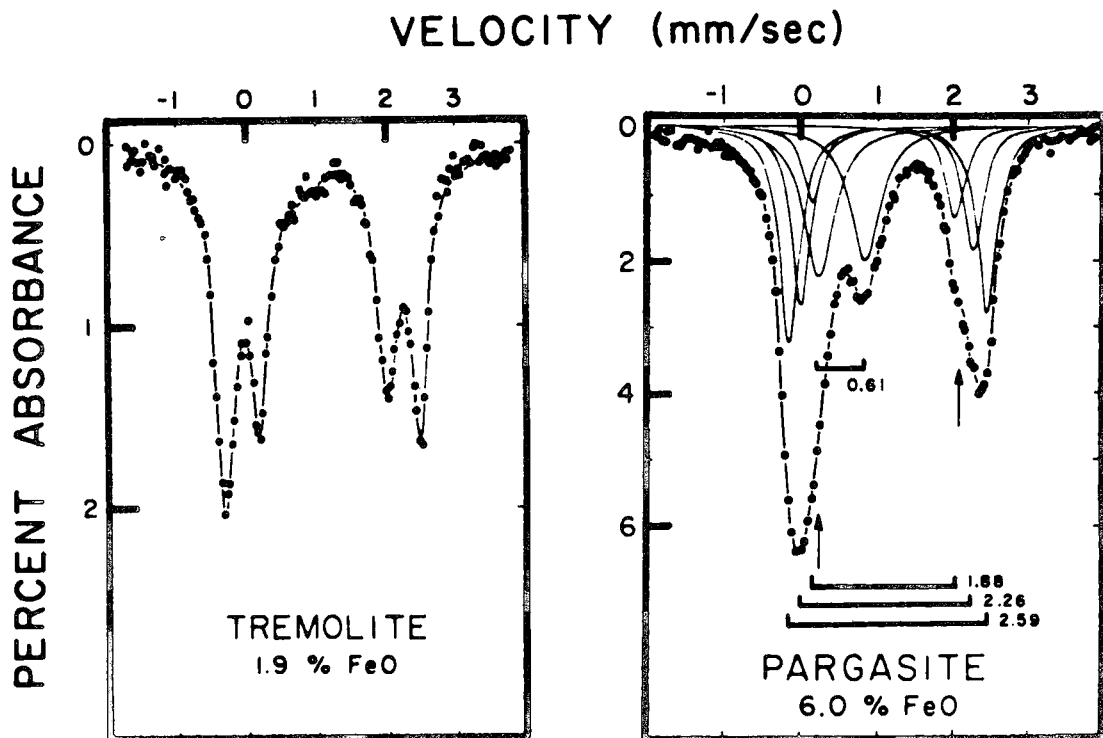
VELOCITY (mm/sec)

FIG. 71. Room-temperature Mössbauer spectra of tremolite (left) and pargasite (right) [from Goldman & Rossman (1977) and Goldman (1979), respectively]. The doublets are assigned as follows. For tremolite outer doublet: Fe^{2+} at $M(1, 2, 3)$, inner doublet: Fe^{2+} at $M(4)$; plus a weak Fe^{3+} doublet. For pargasite, the doublet quadrupole-splitting parameters (mm/s) are shown, and were assigned as follows: 2.59: Fe^{2+} at $M(1, 3)$; 2.26: Fe^{2+} at $M(2)$; 1.88: Fe^{2+} at $M(4)$; 0.61: Re^{3+} predominantly at $M(2)$.

Additional complications occur, as is apparent from the spectrum of pargasite (Fig. 71). This has been resolved into four doublets due to Fe^{3+} (principally at the $M(2)$ site) and Fe^{2+} at $M(1)+M(3)$, $M(2)$ and $M(4)$, respectively. This spectrum is very similar to that of magnesio-hornblende (Fig. 69) and suggests that recognition of an $M(4)$ or an $M(2)$ Fe^{2+} doublet where both are present will be extremely difficult.

Sodic-calcic amphiboles

There has been very little Mössbauer work done on the amphiboles of this group. The spectrum of a synthetic ferro-richterite (Fig. 74) consists of two resolvable doublets due to Fe^{2+} and Fe^{3+}, respectively (Virgo 1972a); the Fe^{2+} doublet consists of three closely overlapping quadrupole-split doublets from Fe^{2+} at the $M(1)$, $M(2)$ and $M(3)$ sites. The spectrum of potassian ferri-taramite(59) can be resolved into three quadrupole-split doublets due to Fe^{2+} at

at $M(1)$, $M(2)$ and $M(3)$, and one quadrupole-split doublet due to Fe^{3+} predominantly at $M(2)$. The predominance of trivalent cations at $M(2)$ would appear to be an important factor in the resolution of the spectrum.

Alkali amphiboles

Mössbauer studies of alkali amphiboles have concentrated on the glaucophane – ferro-glaucophane – magnesio-riebeckite – riebeckite series. In these amphiboles, the $M(2)$ site is generally filled with trivalent cations, and the Mössbauer spectra consist of three quadrupole-split doublets due to Fe^{2+} at $M(1)$ and $M(3)$ and Fe^{3+} predominantly at $M(2)$; typical spectra are shown in Figure 75. The crossite spectrum consists of three doublets, one of which is assigned to Fe^{3+} at $M(2)$ (B,B') and two of which are assigned to Fe^{2+} at $M(1)$ (A,A') and $M(3)$ (C,C'), respectively. The riebeckite spectrum is fairly similar, except that the Fe^{3+} doublet is much stronger than in the crossite spectrum.
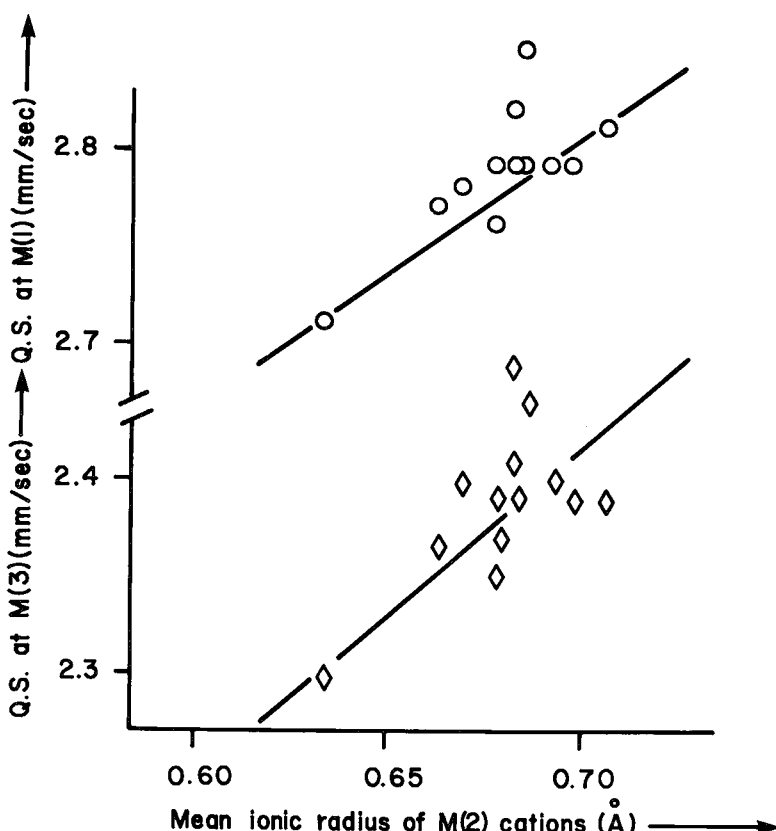
FIG. 72. Some compositional systematics of the Mössbauer parameters in the calcic amphiboles.

Substitution of an actinolite or arfvedsonite component (or both) into riebeckite can give rise to a third Fe^{2+} doublet due to a contribution from Fe^{2+} at M(2).

The systematics of the hyperfine parameters are shown in Figure 76. The quadrupole splitting of Fe^{2+} at M(1) is fairly constant at ~2.80 mm/s, but has greater scatter at larger values of the M(2) cation radius; there does not seem to be any correlation with the M(4) site-occupancy. The quadrupole splitting of Fe^{2+} at M(3) shows a positive correlation with the mean ionic radius of the M(2) cations. In this particular case, the effect of next-nearest-neighbor variation in cation charge is minimized as the M(2) cations are predominantly trivalent and the only variable is cation size, and the M(3) site is remote from the M(4) site where some variation in cation charge does occur. Thus the change in quadrupole splitting of Fe^{2+} at M(3) is due to a change in M(3) polyhedral distortion or a change in the next-nearest-

neighbor cation distances (or both). As was shown previously, the angular distortions of the M(1) and M(3) polyhedra are strongly dependent on the M(2) site-occupancy. Thus increasing cation-size in M(2) causes decreased angular distortion of the M(3) octahedron, which results in increased quadrupole splitting of Fe^{2+} at M(3), in agreement with the deductions of Ingalls (1964). The reason why the quadrupole splitting of Fe^{2+} at M(1) does not exhibit analogous behavior is not clear. There seems to be no systematic variation of isomer shift with composition for Fe^{2+} at M(1) or M(3) in the alkali amphiboles, indicating that there is little or no change in the character of the bonding with changes in composition.

General considerations

A general summary of the variation in Fe^{2+} quadrupole splitting with cation site and amphibole type is given in Figure 77; this should aid
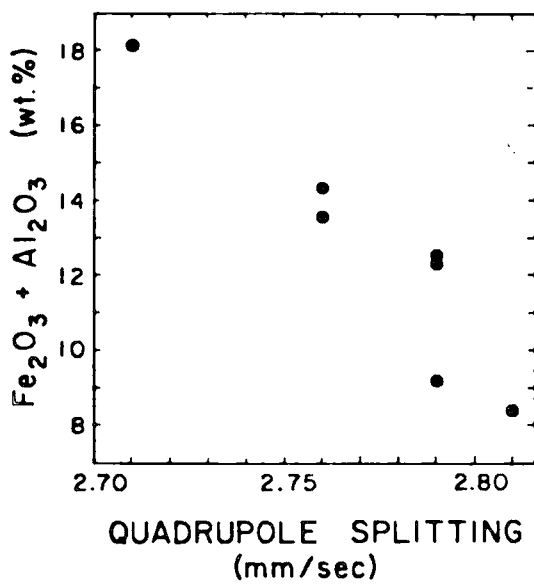
QUADRUPOLE SPLITTING
(mm/sec)

FIG. 73. Variation in quadrupole splitting of the outer Fe^{2+} doublet (AA' in Fig. 69 right) as a function of the $Al_2O_3+Fe_2O_3$ contents of the calcic amphiboles of Bancroft & Brown (1975) [from Goldman (1979)].

peak assignment in the examination of as yet uncharacterized types of amphibole. As is apparent from the above discussion, the refinement and assignment of calcic amphibole spectra are not always straightforward; however, some of the problems can be circumvented by use of a combination of experimental techniques. Recent studies have shown the importance of temperature-dependent electron delocalization in

the analysis of Mössbauer spectra of minerals with mixed valence Fe in adjacent sites (Nolet & Burns 1979, Schwartz et al. 1980). This effect has not yet been documented in amphiboles but is of potential significance in mixed valence Fe-rich amphiboles, and could further complicate spectral interpretation.

INFRARED-ABSORPTION SPECTROSCOPY IN THE OH REGION

The fundamental band of the O–H stretching vibration is in the range 1500–3800 cm^{-1}. The exact position of this band in the infrared region is a function of the strength of the hydrogen-oxygen bond; strong bonds are associated with higher frequencies, the lower end of the range being characteristic of symmetrical hydrogen bonds. In the spectra of amphiboles, the fundamental band occurs from 3600 to 3700 cm^{-1}, indicative of a strong hydroxyl bond and little or no hydrogen bonding; this is compatible with the O(3)–H distance of ~ 1.0 Å found in crystallographic studies. End-member amphiboles show a single sharp stretching band for hydroxyl in this region. However, the principal stretching band in intermediate amphiboles shows considerable fine structure (Fig. 78) that has been attributed to cation substitution effects at those cation sites co-ordinated by the hydroxyl ion. This occurs as a result of the fact that the frequency of the stretching band varies with the actual cations bonded to the hydroxyl. Strens (1974) has shown in the talc structures that the frequency shift is a function of the electronegativity of the bonded cations. Figure 79 shows this also to be the case for the
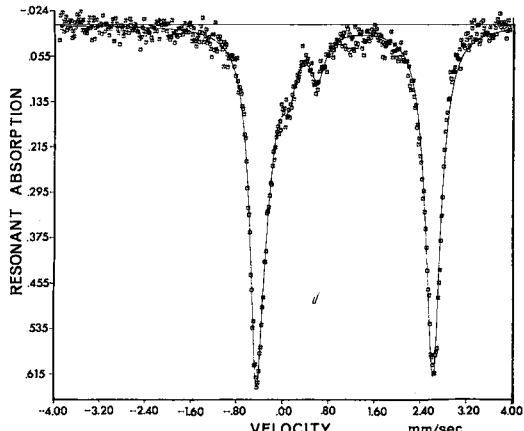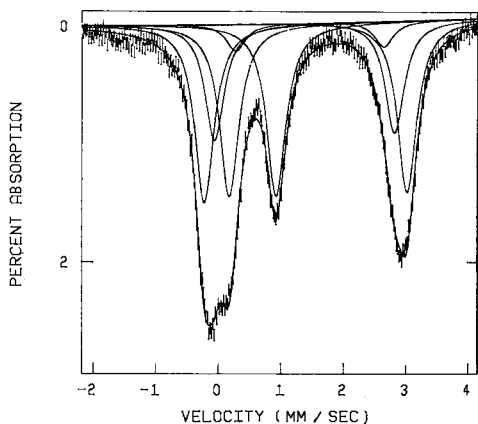

FIG. 74. Mössbauer spectra of richterite (right: liquid nitrogen temperature) and potassian ferri-taramite (left) [from Virgo (1972b) and Hawthorne (1973), respectively].